# Instability of the Superfluid Flow as Black-Hole Lasing Effect

S. Finazzi,[1,*] F. Piazza,[2,†] M. Abad,[3] A. Smerzi,[4] and A. Recati[2,3,‡]
[1]Laboratoire Matériaux et Phénomènes Quantiques, Université Paris Diderot-Paris 7 and CNRS, Bâtiment Condorcet, 10 rue Alice Domon et Léonie Duquet, 75205 Paris Cedex 13, France
[2]Technische Universität München, James-Franck-Straße 1, 85748 Garching, Germany
[3]INO-CNR BEC Center and Dipartimento di Fisica, Università di Trento, 38123 Povo, Italy
[4]QSTAR, INO-CNR and LENS, Largo Enrico Fermi 2, 50125 Firenze, Italy
(Received 15 October 2014; published 17 June 2015)

We show that the critical velocity of a superfluid flow through a penetrable barrier coincides with the onset of the analog black-hole lasing effect. This dynamical instability is triggered by modes resonating in an effective cavity formed by two horizons enclosing the barrier. The location of the horizons is set by $v(x) = c(x)$, with $v(x), c(x)$ being the local fluid velocity and sound speed, respectively. We compute the critical velocity analytically and show that it is univocally determined by the configuration of the horizons. In the limit of broad barriers, the continuous spectrum at the origin of the Hawking-like radiation and of the Landau energetic instability is recovered.

DOI: 10.1103/PhysRevLett.114.245301 PACS numbers: 67.85.-d, 03.75.Hh, 03.75.Kk, 03.75.Lm

*Introduction.*—A very relevant and not fully understood problem in the field of superfluidity is the nature of the decay of the flow past a macroscopic obstacle. On the one hand, it is known how superfluidity decays, namely, via phase slippage induced by nonlinear or topological excitations like solitons or vortices [1]. However, on the other hand, the question why superfluidity breaks down above a certain critical velocity has not yet found a conclusive answer, except from the limiting case where the obstacle is only a small perturbation of a homogeneous flow, in which case the Landau energetic instability takes place.

Because of its high degree of controllability, an optimal system for the investigation of superfluidity is a Bose-Einstein condensate (BEC) of ultracold dilute atoms [2]. In this system, obstacles are created by laser beams which can be precisely controlled over distances of the coherence length. This has allowed the observation of superfluid decay and phase slippage with BECs both with moving obstacles in a bulk [3–6], as well as with obstacles forming a constriction for the flow [7–12]. A quantitative theoretical description of BECs is provided by the Gross-Pitaevskii (GP) equation for the superfluid order parameter $\Psi(\mathbf{r}, t)$. It contains the crucial ingredients giving rise to superfluidity—phase coherence and nonlinearity—and deals with a simple single classical field.

These same favorable features have made it clear that BECs are also suitable to implement analog models of gravity [13,14]. Indeed, first experimental evidences of analog model phenomenology and/or quantum vacuum fluctuations have recently been reported [15–18]. The analog model description not only puts the rich BEC phenomenology into a much broader context, but allows, at the same time, for new predictions and interpretations.

In this Letter, using concepts borrowed from analog models, we show that the supercurrent instability appearing at the critical velocity of the compressible flow through a constriction corresponds to the so-called black-hole lasing effect [19–21]. This provides, on the one side, a deeper understanding of a long standing problem in superfluidity and nonlinear dynamics; on the other side, it allows us to introduce a new setup where the physics of sonic holes emerges naturally.

Focusing on the one-dimensional (1D) flow of a BEC through a penetrable repulsive barrier, we show that the instability governing the underlying saddle-node bifurcation [22,23] is actually a dynamical black-hole lasing effect triggered by a finite set of propagating modes which resonate within an effective cavity formed by two horizons enclosing the obstacle. The position of these sonic horizons is set by $v(x) = c(x)$ (see Fig. 1), with $v(x), c(x)$ being the local flow velocity and sound speed, respectively. Even for a barrier much thinner than the BEC coherence length, the above local quantities are of physical relevance, providing additional negative energy modes inside the cavity where $v(x) > c(x)$. Furthermore, the critical velocity and decay rate depend directly on the configuration of the horizons, and only indirectly on the shape of the barrier and interaction strength [24]; i.e., two very different barriers can give rise to a comparable critical velocity and decay rate, offering a means of experimental testing. For obstacles much broader than the coherence length, one recovers the continuous spectrum of negative energy modes at the basis of Hawking radiation from a single horizon and of the Landau energetic instability, which is triggered by the presence of an impurity in homogeneous supersonic flows.

*Model setup and saddle-node bifurcation.*—A BEC flowing in one direction with a strong transverse confinement can be well described by the 1D GP equation [2]

 

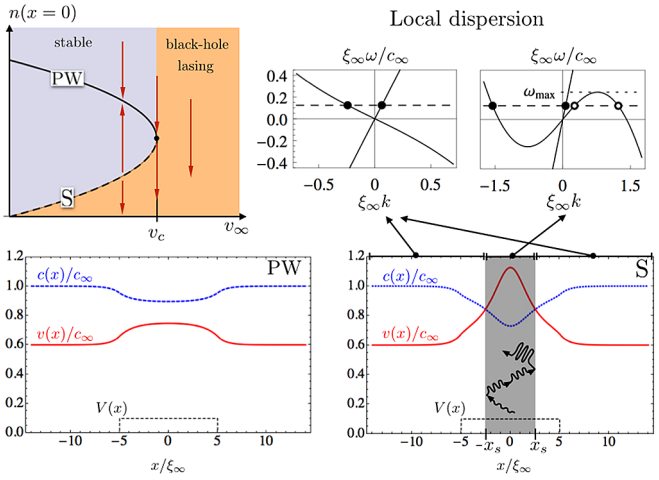


FIG. 1 (color online). Upper left: dynamical phase diagram of the saddle-node bifurcation characterizing the GP equation (1) at fixed injected current. On the vertical axis, the density at the barrier center is reported, distinguishing the PW solution from the other stationary solution S. The arrows indicate the direction of the dynamical evolution, separating a stable region converging toward the PW attractor from an unstable region, delimited by the unstable S solution, where no convergence is present. Lower row: local flow velocity (red solid line) and sound speed (blue dotted line) for the PW and S solutions at a given injected velocity $v = 0.93v_c$, barrier height $V_0 = 0.1gn_\infty$, and width $d = 5\xi_\infty$, with $\xi_\infty$ being the healing length far away from the barrier. Upper right panels: local dispersion relation $[\omega - v(x)k]^2 = c(x)^2k^2 + \hbar^2k^4/4m^2$ of small amplitude modes in the subsonic (left) and supersonic (right) region. The additional modes appearing in the latter propagate back and forth and get amplified, giving rise to the black-hole lasing dynamical instability.

$$i\hbar\partial_t\psi(x,t) = \left(-\frac{\hbar^2}{2m}\partial_{xx} + V(x) + g|\psi(x,t)|^2\right)\psi(x,t), \tag{1}$$

where $\psi(x,t) = \sqrt{n(x,t)}e^{i\phi(x,t)}$ is the superfluid order parameter (or the BEC wave function), $V(x)$ is a repulsive square barrier potential of width $2d$ and height $V_0$, and $g$ is the effective 1D interaction strength. We model the flow by imposing that the density $n = |\psi|^2$ and velocity $v = \hbar\partial_x\phi/m$ take constant values $n_\infty$, $v_\infty$, respectively, far from the barrier at $|x| \to \pm\infty$. This is completely equivalent to solving the GP in a moving frame without the above boundary conditions, which, in turn, describes the case of a moving barrier in a standing BEC [22]. The solutions of the nonlinear Eq. (1) with these boundary conditions show a saddle-node bifurcation [22,23,27–29] at a critical velocity $v_c$ (or barrier height $V_c$), where the only two stationary solutions merge and disappear. These two solutions, shown in the lower panels of Fig. 1, become a plane wave and a soliton when the height of the barrier goes to zero. For this reason, in what follows, we shall refer to them as the plane wave (PW) solution and the soliton (S) solution. As indicated by the arrows in the upper left panel of Fig. 1, the PW solution is a stable attractor within the parameter region delimited by the S solution. As verified numerically with GP dynamics [22] and linear stability analysis [23,30], the latter is, instead, dynamically unstable. This unstable behavior, characterized by soliton emission, is also present in the whole region above $v_c$, where the emitted solitons belong to a nonlinear dispersive shock-wave [22,31,32]. The dynamical saddle-node phase diagram of the upper left panel in Fig. 1 can be modeled by the equation $\dot{f}(t) = (v_c - v) - f^2(t)$, where the unstable region corresponds to a function $f$ diverging in time $t$. This simple model also explains the universality of the dynamics on all sides of the bifurcation, which has been verified numerically in [23].

*The black-hole lasing effect.*—In the following, we show that the dynamical instability characterizing the GP saddle-node bifurcation and, thereby, responsible for the superflow decay, is due to the black-hole lasing effect, whose origin is the presence of a black-hole–white-hole pair of sonic horizons. For this purpose, we study perturbations on top of the stationary solutions by means of the Bogoliubov-de Gennes equation. The latter can be written in terms of the flow velocity $v(x)$ and local speed of sound $c(x) = \sqrt{gn(x)/m}$ only [25]. Therefore, the excitation spectrum and the presence and the nature of any instability are fully governed by $v(x)$ and $c(x)$. Remarkably, this property, which allows for the mapping to the Klein-Gordon equation describing the propagation of a scalar field on a curved spacetime [26], holds even when the local density description of the flow breaks down, i.e., even when the healing length $\xi(x) = \hbar/2mc(x)$ exceeds the barrier width.

As it appears from the lower right panel of Fig. 1, the S solution always presents two sonic horizons at $x = \pm x_s$, delimiting a compact supersonic region where the local flow velocity exceeds the sound speed. Thus, the point $-x_s < 0$ such that $v(-x_s) = c(-x_s)$ behaves as the analog of a black-hole horizon, in the sense that phonons cannot propagate from the internal to the external region. Similarly, the point $+x_s$ such that $v(x_s) = c(x_s)$ is the analog of a white-hole horizon. In particular, when the distance between the horizons is large enough, the spectrum of perturbations is enriched by additional propagating modes characterized by a negative norm, thus, carrying negative energy as seen by the laboratory reference frame (the general case of arbitrarily small distance between the horizons is discussed below). As shown in Fig. 1, the Bogoliubov dispersion relation

$$(\omega - vk)^2 = c^2k^2 + \frac{\hbar^2k^4}{4m^2} \tag{2}$$

admits, indeed, only two real solutions of the wave number $k$ for each frequency $\omega$ in the subsonic region, corresponding to two standard leftward and rightward propagating

modes. Instead, in the supersonic region, it has four real solutions for $\omega$ smaller than a certain threshold frequency $\omega_{\max}$, two of them (open dots) lying on the negative-norm branch of the dispersion relation. These bounded anomalous modes give rise to anomalous transmission and reflection, ultimately leading to a cavity amplification effect generating a dynamical instability known as black-hole laser effect [19–21,33–36]. More precisely, Hawking-like phonons are emitted by the analog horizons $x = \pm x_s$ [37] due to the anomalous scattering of negative- and positive-norm modes. These horizons act as amplifiers of phonons [38], converting a negative-norm wave of unitary amplitude into two negative- and positive-norm waves of amplitudes $\alpha$ and $\beta$, respectively, with $|\alpha|^2 - |\beta|^2 = 1$ and $|\alpha| > 1$. Since the supersonic region is compact, the negative-norm waves, one left going and one right going, are trapped and can be interpreted as a single mode bouncing back and forth between the two sonic points. Consequently, the internal region acts as a resonant cavity for this mode which exponentially grows being amplified at any bounce on the sonic horizons. Formally, this leads to the appearance of positive imaginary parts in the Bogoliubov frequency spectrum.

However, when the horizons are close to each other, a naive analysis of the dispersion relation Eq. (2) is not sufficient to properly describe the properties of the spectrum of these modes. Still, our results also apply to this case. As shown below, one can, indeed, derive a generalized Bohr-Sommerfeld quantization condition which fixes the number of resonant negative-norm cavity modes, their frequencies, and growing rates. Accordingly, negative energy modes can appear only if at least one oscillation can be hosted within the two classical turning points $\pm x_s$ of the Bogoliubov-de Gennes equation. Thus, the presence of a region with $c(x) \leq v(x)$ is necessary but not sufficient for existence of negative energy modes. Remarkably, the appearance of negative energy modes in a compact supersonic region has been experimentally verified using Bragg spectroscopy [15].

In the following, we provide the main results of our calculations, which are presented in detail in the Supplemental Material (SM) [39]. We generalize the methods developed in [20,21,43–45] for steplike flow profiles with constant velocity to the physically relevant configuration (see Fig. 1) discussed in the present Letter. It can be shown that, when the fluid velocity is increased, the first unstable mode appears at $\omega = 0$. When the flow is symmetric with respect to $x = 0$ (more general cases are considered in the SM [39]), this implies that the flow is unstable when

$$\frac{2m}{\hbar}\int_{-x_s}^{x_s} dx \sqrt{v(x)^2 - c(x)^2} \geq \arg\frac{\beta}{\alpha}. \tag{3}$$

The left-hand side of this inequality is the phase acquired by a zero-frequency mode propagating across the supersonic region. The right-hand side is, instead, associated to the phase acquired by the mode when scattered at the sonic point.

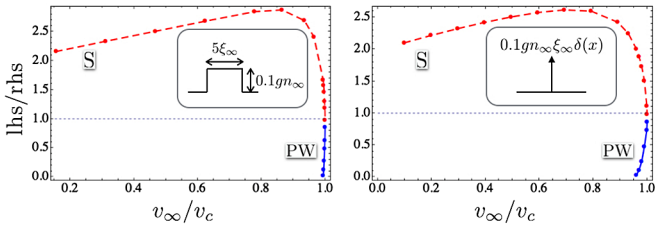


FIG. 2 (color online). Ratio between the left- and the right-hand sides of Eq. (3) for the PW (blue dots with solid line) and S (red dots with dashed line) solutions in the hydrodynamic regime (left panel, parameters as in the lower panels of Fig. 1) and for the delta barrier potential [right panels, $V = 0.1gn_\infty\xi_\infty\delta(x)$].

The ratio of the two sides of this inequality is reported in Fig. 2 for the PW (blue dots with solid line) and S solutions (red dots with dashed line) in the hydrodynamic regime (left panel) and for a delta barrier potential (right panel). This ratio is always smaller than one for the PW solution, which, therefore, never supports a cavity mode, while it is greater than the one for the S solution, which, then, always supports a cavity mode. The main result is that, at the bifurcation point, both solutions reach the marginal condition for the appearance of the cavity mode. Moreover, the condition Eq. (3) allows for an analytical prediction of the critical velocity $v_c$ corresponding to the bifurcation point. In the case where the fluid velocity and the speed of sound assume steplike profiles, i.e., $v_\infty = v(|x| > x_s)$, $v_{\rm barr} = v(|x| < x_s)$ and the same for $c(x)$, the results of Ref. [43] are recovered and the critical injected velocity $v_c$ is obtained by solving

$$\frac{2mx_s}{\hbar}\sqrt{v_{\rm barr}^2 - c_{\rm barr}^2} = \arctan\frac{\sqrt{v_{\rm barr}^2 - c_{\rm barr}^2}\sqrt{c_\infty^2 - v_\infty^2}}{v_{\rm barr}v_\infty - \lambda c_{\rm barr}^2}, \tag{4}$$

for $v_\infty$, and $\lambda = [1 + \ln(v_\infty/v_{\rm barr})]/[1 - \ln(v_\infty/v_{\rm barr})]$. The most general formula valid for any smooth profile is derived in the SM [39]. Note that the resulting critical velocity depends on the barrier potential $V$ and on the coupling $g$ only through the local sound speed and flow velocity, according to the adopted analog gravity description. Since $v(x)$ and $c(x)$ always vary on scales larger than or comparable to the healing length, this condition can be applied even to very narrow potential barriers, as illustrated in the right panel of Fig. 2 in the case of a delta potential.

As anticipated, the anomalous cavity modes are always dynamically unstable, having positive imaginary parts $\Gamma_n$ of the complex eigenfrequencies. Typical results, computed using the algorithm developed in Ref. [21] are presented in Fig. 3. In the upper panels, the blue dots represent the value of the cavity mode amplitude $|B|^2$ as a function of energy $\omega$ and for two different cavity lengths $2x_s$.

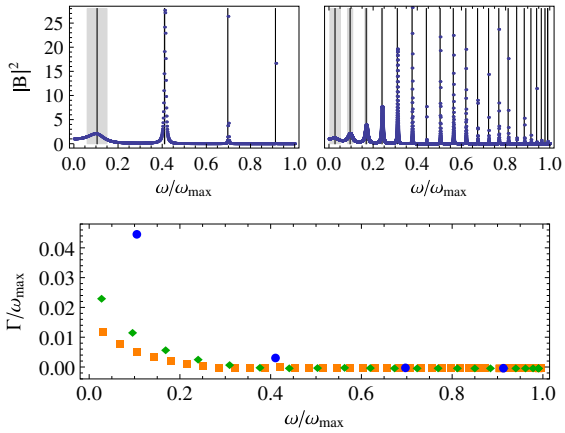


FIG. 3 (color online). Upper panels: Squared modulus of the amplitude $B$ of the cavity mode (blue dots) for a unitary incoming left-going wave for two values of the distance $2x_s$ between the sonic points ($2x_s/\xi_s = 10$, left; $2x_s/\xi_s = 50$, right). Vertical lines denote the real parts of the complex eigenfrequencies $\omega_n + i\Gamma_n$ and the shaded areas represent the intervals $(\omega_n - \Gamma_n, \omega_n + \Gamma_n)$. Lower panel: Spectra for $2x_s/\xi_s = 10, 50, 100$ (blue dots, green diamonds, orange squares). For $2x_s \to \infty$, $\Gamma_n \to 0$ and the spectrum becomes dense in the real interval $(0, \omega_{max})$.

In the lower panel, the imaginary part is shown. As the cavity width $2x_s$ grows, the number of eigenfrequencies increases while their imaginary parts vanish, such that the spectrum becomes dense in the real interval $(0, \omega_{max})$. Thus, for $x_s \to \infty$, phonons are spontaneously emitted for all frequencies $\omega < \omega_{max}$, the emission rate is constant in time ($\Gamma_n = 0$), and the instability is energetic rather than dynamical. In this limit, two different mechanisms can excite the same continuous set of negative-energy modes: (i) Hawking-like pairs of phonons are emitted from each of the two far apart sonic horizons [25]; (ii) In the presence of impurities, phonons are produced by Landau instability. In this regime, achievable with a broad potential such that $2x_s \gg \xi_s$, the critical condition corresponds to the flow velocity reaching the sound speed inside the barrier region, which, in our one-dimensional configuration, means $v(x = 0) = c(x = 0)$. This criterion has been numerically verified in the hydrodynamic regime of the GP equation in one [46], two [47–50], and three dimensions [51–53] and, also, for a fermionic superfluid using the Bogoliubov-de Gennes equations [54], as well as in the toroidal BEC experiments of [10,12].

*Conclusions.*—By showing that the instability of the one-dimensional BEC flow through a penetrable barrier is due to the dynamical black-hole lasing effect, this work builds a bridge between field theory in curved spacetime and superfluidity. It provides a deeper insight into the long-standing problem of supercurrent instability and also identifies an experimental available setup as a natural candidate for observing interesting physics of fluctuations in curved spacetime.

In particular, we have shown that the behavior of the system is governed by the configuration of the sonic horizons and the (mis)match in the number of excitation modes on the two sides of them. This allowed us to provide a general formula predicting the critical velocity and to characterize the crossover between the dynamical black-hole lasing instability and the Hawking energetic instability. The latter coincides with the well-known Landau instability and is achieved for broad enough barrier potentials.

The present analysis also allows for a suggestive explanation of the known supercritical stationary flow, found for velocities $v_\infty$ larger than a second higher critical velocity [7,32,55]. For this stationary configuration, the flow at the barrier is slower than outside. If $v_\infty$ is large enough, the flow will be everywhere supersonic [32] and, at low frequencies, there will be four propagating modes both in the internal and the external regions [56]. If $v_\infty$ is maintained supersonic but decreased below this higher critical velocity, the internal region may become subsonic. In this case, phonons are expected to be emitted with a linearly growing rate, as suggested by studies in the context of Lorentz violating quantum field theories [57].

Our study does not include the possibility for fluctuations (thermal or quantum) to trigger the instability of the PW branch before the critical saddle-node bifurcation point is reached. However, the black-hole lasing instability should be the relevant decay mechanism also in this case. Indeed, it has been shown [58] that fluctuations lead the stable PW branch to tunnel into the unstable S solution. It is the dynamical instability of the latter, which we have shown to be due to black-hole lasing, that leads to soliton emission.

An extension of this study to the two- or three-dimensional flow, where a more complicated horizon configuration appears, would be the object of future study.

We are grateful to N. Pavloff and J. Steinhauer for very useful comments. We thank I. Carusotto and O. Gat for stimulating discussions. This work has been financially supported by ERC through the QGBE grant and by Provincia Autonoma di Trento. A. R. and F. P. acknowledge support from the Alexander Von Humboldt foundation.

*Note added.*—Experimental evidence of black-hole laser effect has been very recently reported by Jeff Steinhauer in Ref. [59].

*Present address: Mario Negri Institute for Pharmacological Research, Villa Camozzi, 24020 Ranica, Italy.
stefano.finazzi@marionegri.it
†francesco.piazza@ph.tum.de
‡recati@science.unitn.it

[1] P. W. Anderson, Rev. Mod. Phys. **38**, 298 (1966).
[2] L. P. Pitaevskii and S. Stringari, *Bose-Einstein Condensation* (Clarendon Press, Oxford, 2003).

[3] C. Raman, M. Köhl, R. Onofrio, D. S. Durfee, C. E. Kuklewicz, Z. Hadzibabic, and W. Ketterle, Phys. Rev. Lett. **83**, 2502 (1999).

[4] R. Onofrio, C. Raman, J. M. Vogels, J. R. Abo-Shaeer, A. P. Chikkatur, and W. Ketterle, Phys. Rev. Lett. **85**, 2228 (2000).

[5] T. W. Neely, E. C. Samson, A. S. Bradley, M. J. Davis, and B. P. Anderson, Phys. Rev. Lett. **104**, 160401 (2010).

[6] R. Desbuquois, L. Chomaz, T. Yefsah, J. Lonard, J. Beugnon, C. Weitenberg, and J. Dalibard, Nat. Phys. **8**, 645 (2012).

[7] P. Engels and C. Atherton, Phys. Rev. Lett. **99**, 160405 (2007).

[8] S. Levy, E. Lahoud, I. Shomroni, and J. Steinhauer, Nature (London) **449**, 579 (2007).

[9] A. Ramanathan, K. C. Wright, S. R. Muniz, M. Zelan, W. T. Hill, C. J. Lobb, K. Helmerson, W. D. Phillips, and G. K. Campbell, Phys. Rev. Lett. **106**, 130401 (2011).

[10] S. Moulder, S. Beattie, R. P. Smith, N. Tammuz, and Z. Hadzibabic, Phys. Rev. A **86**, 013629 (2012).

[11] C. Ryu, P. W. Blackburn, A. A. Blinova, and M. G. Boshier, Phys. Rev. Lett. **111**, 205301 (2013).

[12] K. C. Wright, R. B. Blakestad, C. J. Lobb, W. D. Phillips, and G. K. Campbell, Phys. Rev. A **88**, 063633 (2013).

[13] C. Barceló, S. Liberati, and M. Visser, Classical Quantum Gravity **18**, 1137 (2001).

[14] P. B. Blakie and F. Beyer, Ann. Phys. (Amsterdam) **525**, A163 (2013).

[15] O. Lahav, A. Itah, A. Blumkin, C. Gordon, S. Rinott, A. Zayats, and J. Steinhauer, Phys. Rev. Lett. **105**, 240401 (2010).

[16] J.-C. Jaskula, G. B. Partridge, M. Bonneau, R. Lopes, J. Ruaudel, D. Boiron, and C. I. Westbrook, Phys. Rev. Lett. **109**, 220401 (2012).

[17] J. Armijo, Phys. Rev. Lett. **108**, 225306 (2012).

[18] C.-L. Hung, V. Gurarie, and C. Chin, Science **341**, 1213 (2013).

[19] S. Corley and T. Jacobson, Phys. Rev. D **59**, 124011 (1999).

[20] A. Coutant and R. Parentani, Phys. Rev. D **81**, 084042 (2010).

[21] S. Finazzi and R. Parentani, New J. Phys. **12**, 095015 (2010).

[22] V. Hakim, Phys. Rev. E **55**, 2835 (1997).

[23] C.-T. Pham and M. Brachet, Physica (Amsterdam) **163D**, 127 (2002).

[24] This is a general feature of systems described by the Bogoliubov-de Gennes equation, which can always be written only in terms of $v(x)$ and $c(x)$. This property is also at the basis of the analogy between the propagation of sound in a superfluid and of a scalar field in a curved space-time exploited in analog gravity applications [25,26].

[25] J. Macher and R. Parentani, Phys. Rev. A **80**, 043601 (2009).

[26] C. Barcelo, S. Liberati, and M. Visser, Living Rev. Relativity **14**, 3 (2011).

[27] A. Baratoff, J. A. Blackburn, and B. B. Schwartz, Phys. Rev. Lett. **25**, 1096 (1970).

[28] F. Sols and J. Ferrer, Phys. Rev. B **49**, 15913 (1994).

[29] F. Piazza, L. A. Collins, and A. Smerzi, Phys. Rev. A **81**, 033613 (2010).

[30] S. Watabe and Y. Kato, Phys. Rev. A **88**, 063612 (2013).

[31] A. V. Gurevich and L. P. Pitaevskii, Sov. Phys. JETP **38**, 291 (1974).

[32] A. M. Leszczyszyn, G. A. El, Y. G. Gladush, and A. M. Kamchatnov, Phys. Rev. A **79**, 063608 (2009).

[33] C. Barceló, A. Cano, L. J. Garay, and G. Jannes, Phys. Rev. D **74**, 024008 (2006).

[34] U. Leonhardt, T. Kiss, and P. Öhberg, Phys. Rev. A **67**, 033602 (2003).

[35] U. Leonhardt and T. G. Philbin, arXiv:0803.0669.

[36] P. Jain, A. S. Bradley, and C. W. Gardiner, Phys. Rev. A **76**, 023617 (2007).

[37] L. J. Garay, J. R. Anglin, J. I. Cirac, and P. Zoller, Phys. Rev. Lett. **85**, 4643 (2000).

[38] W. G. Unruh, arXiv:1107.2669.

[39] See Supplemental Material at http://link.aps.org/supplemental/10.1103/PhysRevLett.114.245301 for a detailed derivation of the results presented in this Letter, which includes Refs. [40–42] .

[40] N. D. Birrell and P. C. W. Davies, *Quantum Fields in Curved Space* (Cambridge University Press, Cambridge, England, 1984).

[41] C. Mayoral, A. Fabbri, and M. Rinaldi, Phys. Rev. D **83**, 124047 (2011).

[42] S. Finazzi and R. Parentani, Phys. Rev. D **85**, 124027 (2012).

[43] F. Michel and R. Parentani, Phys. Rev. D **88**, 125012 (2013).

[44] S. Finazzi and R. Parentani, Phys. Rev. D **83**, 084010 (2011).

[45] A. Coutant and R. Parentani, Phys. Rev. D **90**, 121501 (2014).

[46] G. Watanabe, F. Dalfovo, F. Piazza, L. P. Pitaevskii, and S. Stringari, Phys. Rev. A **80**, 053602 (2009).

[47] T. Frisch, Y. Pomeau, and S. Rica, Phys. Rev. Lett. **69**, 1644 (1992).

[48] T. Winiecki, B. Jackson, J. F. McCann, and C. S. Adams, J. Phys. B **33**, 4069 (2000).

[49] A. C. Mathey, C. W. Clark, and L. Mathey, Phys. Rev. A **90**, 023604 (2014).

[50] F. Piazza, L. A. Collins, and A. Smerzi, Phys. Rev. A **80**, 021601 (2009).

[51] F. Piazza, L. A. Collins, and A. Smerzi, New J. Phys. **13**, 043008 (2011).

[52] F. Piazza, L. A. Collins, and A. Smerzi, J. Phys. B **46**, 095302 (2013).

[53] D. L. Feder, C. W. Clark, and B. I. Schneider, Phys. Rev. A **61**, 011601 (1999).

[54] A. Spuntarelli, P. Pieri, and G. Strinati, Phys. Rep. **488**, 111 (2010).

[55] N. Pavloff, Phys. Rev. A **66**, 013610 (2002).

[56] S. Finazzi and R. Parentani, J. Phys. Conf. Ser. **314**, 012030 (2011).

[57] A. Coutant, S. Finazzi, S. Liberati, and R. Parentani, Phys. Rev. D **85**, 064020 (2012).

[58] J. A. Freire, D. P. Arovas, and H. Levine, Phys. Rev. Lett. **79**, 5054 (1997).

[59] J. Steinhauer, Nat. Phys. **10**, 864 (2014).